



Modeling Asthma-Prone Areas Using Machine Learning

Jyoti Mishra, Department of Computer Applications, Manipal University Jaipur, Jaipur, India jyoti.sl15@gmail.com
 Dr. Shailendra Shukla, Professor, Department of Mathematics, Arya PG College, Jaipur, India shailjpr41184@gmail.com

ABSTRACT

Asthma prevalence is currently rising sharply as a result of population growth, rising environmental pollutants, and changing lifestyles. As a result, the goal of this study was to locate Tehran, Iran's asthmatic areas by taking both environmental and geographic aspects into account. Data from 872 locations in children who have asthma and 13 ecologic factors that affect illnesses (distance to play areas and roadways, weather patterns, temperature, humidity, air pressure, wind speed, particulates (PM 10 & PM 2, 5), ozone (O3), Sulfur Dioxide (SO2), Carbon Monoxide (CO), and Nitrogen Dioxide (NO2)) were collected in order to map asthma-prone areas (NQ). According to the findings of the spatial autocorrelation and RF model, the reference distances to parks and roads, as well as the levels of PM 2.5 and PM 10, had the strongest impact on the prevalence of asthma in the study area. A geographical autocorrelation study revealed that there was no randomness in the distribution of asthma cases. The results of the receiver performance characterization show how highly accurate the RF model is (the area under the curve was between 0.987 and 0.921 for the training and test data, respectively).

I. INTRODUCTION

Today, as society develops, diseases become more varied and affect more individuals. Asthma is one of the most common ailments. People with asthma have immune systems that react more severely than usual to seemingly benign elements in their daily environment. Each year, there are 5% more asthmatics than there were the previous year. Due to pollution from environmental irritants, childhood asthma cases have sharply grown during the past 50 years in modern, affluent nations. Asthma already affects 300 million people globally, with 400 million people estimated to have the condition by 2025, Recent World Health Organization (WHO) research indicates. In Iran, chronic non-communicable diseases caused about 82% of fatalities in 2015; 4% of these deaths were attributable to respiratory conditions. Asthma is more common in Tehran Province than in other Iranian provinces, with 12.6% of children aged 6-7 and 16.6% of children aged 13-14 reporting asthma. Tehran has a greater rate of asthma prevalence than the rest of Iran on average, which can be attributed to a multitude of asthma-related conditions, including Tehran province's high levels of air pollution. Asthma is so widespread that, if untreated and unmanaged, it might pose a major threat to the public's health.

This disease can develop and worsen due to a number of variables that depend on geographic location, environmental factors, and personal lifestyle choices. The best strategy to prevent allergies is to identify allergens and minimize exposure to them. Finding the environmental factors that affect the occurrence of asthma can help to lessen its effects because a substantial number of these elements are connected to the environment of humans. Therefore, by obtaining pertinent information about people's living surroundings, it is possible to quantify the contribution of various environmental factors to the start and course of this condition.

Using Geographic Information System (GIS) technology is especially useful for figuring out the relationship between illness incidence and environmental quality. GIS could be used for illness prediction, surveillance, and epidemic control by processing health data, examining geographic distribution, and producing maps. Site-based analyses are useful for carrying out epidemiologic studies of asthma risk factors (exposures), for finding areas where the disease is more common, and for diagnosing and treating the condition. Numerous research have used GIS to spatially investigate asthma to date. Hashimoto et al. In Tokyo, Japan, we looked at how the weather affected emergency asthma patients.

In order to map asthma-prone zones in Tehran, Iran, this study used RF models and environmental parameters. Given the environmental elements that influence asthma .The



current work is novel in that it deploys a machine learning HF model in conjunction with his GIS to identify asthma-prone zones.

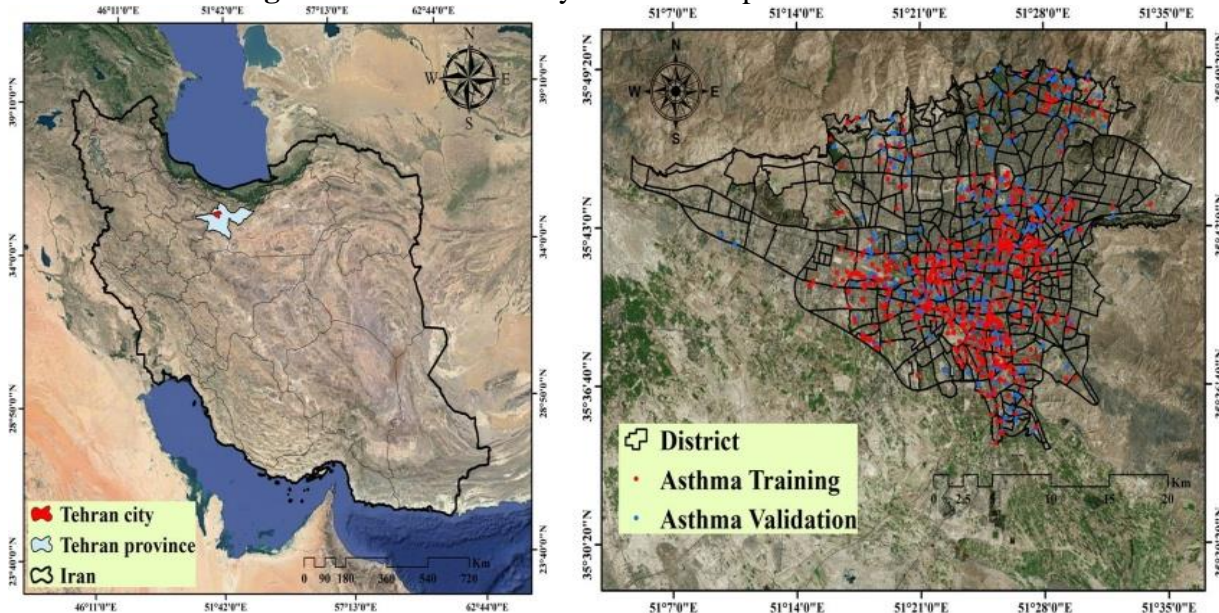
II. METHODOLOGY

There were five steps in the research process. Using the locations of asthmatic kids and the 13 environmental asthma triggers, a spatial database was first generated. In a subsequent stage, the geographical correlations between asthma patients and environmental factors were ascertained using a Model of frequency ratio (FR). The physical autocorrelation of asthma frequency was investigated in a third step. In the fourth step, asthma risk areas were located using the RF model. In the last stage, the modelling was evaluated using sensitivity analysis and receiver operating characteristic (ROC) curves.

Survey Area

Iran's capital, Tehran, has a population of 8,693,706 people. 24th in the world and first in West Asia for population. Tehran has a 730 km² surface area and is situated at 35°36'N and 51°17'E and 51°39'E longitude. Sea level from north to south, sea level drops. One of Tehran's biggest environmental issues is air pollution, which is caused by the city's geographic location, mountains, traffic, z enclosure effects, and pollution from cars, motorcycles, gas stations, and industry. Tehran's location is seen in Fig. 1.

Figure1. Area under study with asthma patients' locations.



SPATIAL DATABASE

The first step was to create a spatial database with independent dependent datasets. Her 2019 asthmatic children's location in Tehran was among the pertinent information. This information is derived from the Hospital Information System, which has 872 cases and is one of the major facilities offering medical care for respiratory disorders. Asthma location data were used for modelling in 70% (611 cases) and analysis in 30% (261 instances) (see Figure 1). Environmental factors that affect asthma have been found in WHO reports and earlier studies. O₃, CO, NO₂, SO₂, Some of these factors are PM 10, PM 2.5, climatic factors (precipitation, temperature, humidity, pressure, and wind speed), the distance to roads, and the distance to parks. Included. The Tehran Air Pollution Management Company's 23 pollution monitoring stations were used to gather data on air pollution. Annual averages of these metrics from 2009 to 2019 were used for this purpose. Using these attributes' annual averages from 12 weather stations in the province of Tehran between 2009 and 2019, a map of meteorological parameters was created. Kriging interpolation was used to map air pollution and meteorological features in the ArcGIS 10.3 environment. Standards for walking distances to parks and roads were established using the Tehran land-use map. Environmental variables affecting asthma conditions are shown in Fig. 2.

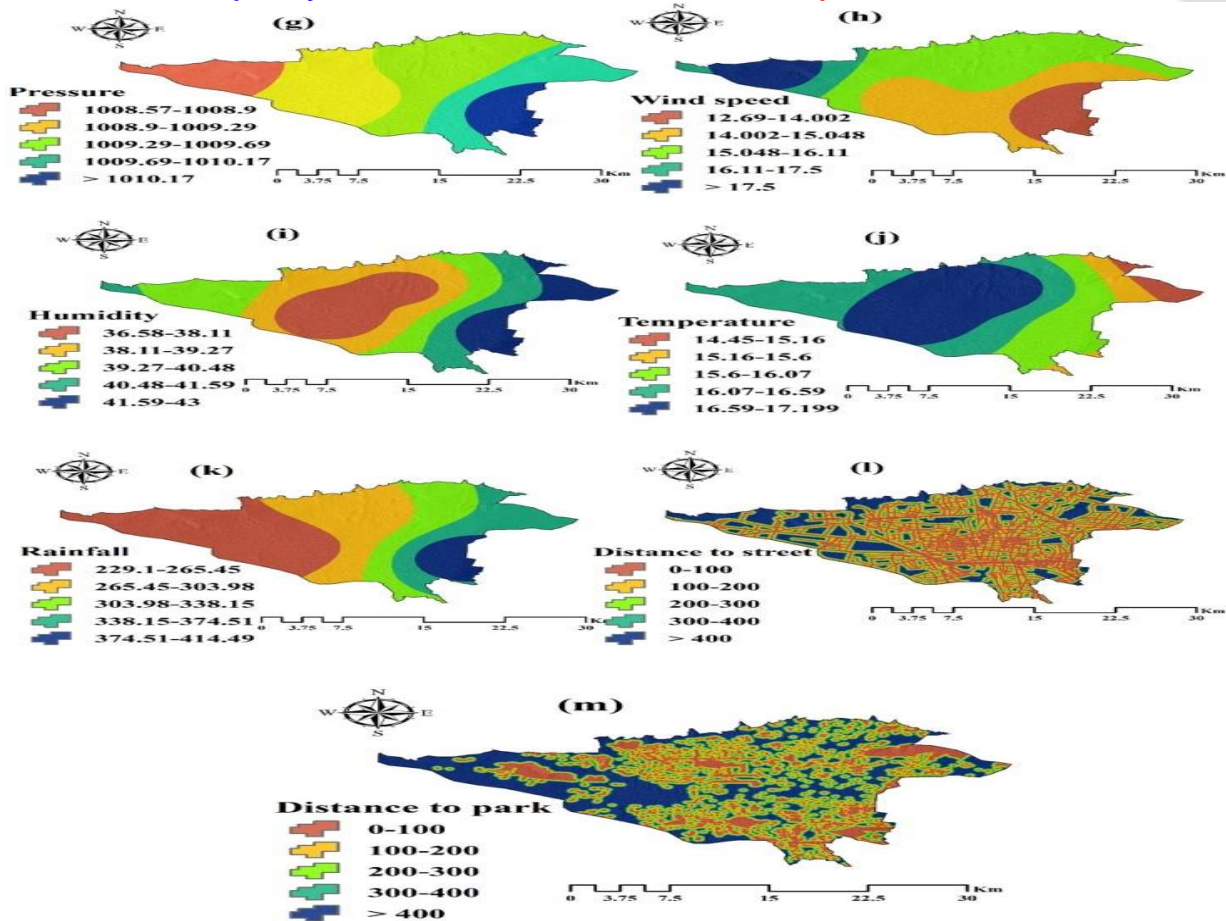


Figure2. Environmental factors that influence

asthma. Grainy matter Specifically, PM 10, PM 2.5, CO, O3, SO2, NO2, CO, O3, and The following factors are taken into consideration: (g) pressure, (h) wind speed, (I) humidity, (j) temperature, (k) rainfall, (l) distance to street, and (m) distance to parking. ESRI, Redlands, California, USA, <http://www.esri.com>, ArcGIS 10.3 was used to create this map.

Moran’s I index

One technique for assessing the spatial autocorrelation between spatial data is this index. Moran's I in the dataset range from -1 to +1 If the Moran's I index value is greater than 0, then there is positive spatial autocorrelation. If less than zero, negative. There is no spatial autocorrelation when it is near to zero. Eq. (1) is used to calculate the Moran's I index.

$$I = \frac{\sum_{i=1}^N \sum_{j=1}^N w_{ij} (x_i - \bar{x})(x_j - \bar{x})}{\sum_{i=1}^N (x_i - \bar{x})^2}$$

where x represents the average number of asthma cases, N represents the overall number of asthma cases, wij represents the spatial weight between polygons I and j, and xi and xj represent the numbers of asthma cases in each of the two polygons, respectively.

This analysis examines the relationship between points and neighbors in the local Moran's I index, where four scenarios are possible:

- High- High (H -H): When the spatial autocorrelation of a value and its contemporaries are both positive. When one is positive and the other is negative, it is said to be high-low (H-L).
- Low - High (L-H): the condition in which the former is negative and the latter is positive.
- Low-Low (L-L): When the first and last are equally negative

Getis- Ord Gi* index

This index examines the accumulation of extraordinarily large or extremely small amounts



of the occurrence of an event and includes signs of hot spots (areas of high risk) and cold spots (low-risk areas). Positive or negative Z-score values indicate hot or chilly locations, respectively²⁹. The Getis-Ord G_i^* index is calculated using Eq. (2).

$$\gamma(h) = \frac{1}{2N(h)} \sum_{i=1}^{N(h)} [Z(x_i) - Z(x_i + h)]^2$$

$$G = \left(\frac{\sum_{i=1}^N \sum_{j=1}^N w_{ij} x_i x_j}{\sum_{i=1}^N \sum_{j=1}^N x_i x_j} \right)$$

x_i and x_j represent the numbers of occurrences in polygons I and j , respectively, while w_{ij} represents the spatial weight between polygons I and j . N is the total number of asthma cases.

SEMIVARIOGRAM

The Free Encyclopedia

The ability of a semi variogram to identify variables' spatial coherence is well established. It is thought that a mathematical model known as a semi variogram can accurately depict the reliance between samples. Spatial coherence is the concept that adjacent samples are mutually dependent to a specific distance. Using Eq.(3), a semi-variogram is calculated.

Where $Z(x_i)$ stands for the sample value at point x_i , $Z(x_i+h)$ stands for the sample value at point x_i+h , h stands for the distance in the specified direction between position x_i and x_i+h , $N(h)$ stands for the number of pairs of samples that are at a distance of h from one another, $\gamma(h)$ stands for the value of the semi-variogram for distance h , and $Z(x_i)$.

Range, threshold, and nugget are the three parameters of a semi variogram and are defined as follows:

Still: The constant value of the variogram over the permitted range. The value of the façade change was calculated by summing the variances of each sample used to calculate it.

Nugget: The variogram's origin value is the nugget. In other words, if $h = 0$, its value should ideally be 0.

Equation (4) is used to obtain the optimal correlation using the spatial dependence index from equation (1).

$$SD = \frac{\text{nugget}}{\text{nugget} + \text{partialsill}} \times 100$$

It denotes a strong spatial correlation when it is less than 25%, a moderate spatial correlation when it is between 25% and 75%, and a weak spatial correlation when it is greater than 75%.

FR- Model



The FR model introduces the collection of training points as the dependent variable and the variables influencing asthma as the independent variables. This model determines the probability that asthma will occur in each class based on all criteria. Each variable is evaluated independently of the formula used in order to determine the impact of each class.

$$FR = \frac{F_i}{P_i}$$

where F_i is the fraction of training points that are placed in class I P_i is the percentage of class I pixels over the total study region, and FR is the influence of each class on each parameter.

RF Model

Breiman proposed the RF model as a cumulative learning method based on decision trees for grouping and regression challenges.. A group of unpruned trees obtained by means of a recursive segmentation technique make up RF. A collection of trees based on N different



observations are used to generate the RF. This model consists of numerous decision trees, each of which was constructed using a different random set of input variables and various bootstrap instances of the data. The bootstrap method is used to sample and place a number of N samples from the main observation data set. The remaining one-third of the data, known as out-of-process samples, is not sampled during the sampling procedure. Add the test data to the trees once they have all been built to find out how many trees there are given the input vector. The final result is calculated by averaging this output.

III. Validation

The modelling of asthma-prone areas was evaluated in this case using the ROC index, area under the curve (AUC), mean-absolute error (MAE), and sensitivity analysis.

ROC Curve

Two sensitivity axes (x-axis) and one transparency axis make up the ROC curve (y-axis). The formulas provide these axes. The comparison matrix with threshold definitions between 0 and 1 yields (6) and (7).

Eq (6)

$$X = 1 - \left[\frac{TN}{TN + FP} \right]$$

Eq(7)

$$Y = \left[\frac{TP}{TP + FN} \right]$$

where TP denotes pixels that were correctly assigned to the category of interest, TN denotes pixels that were wrongly assigned, FP denotes pixels that were assigned incorrectly, and FN denotes pixels that were assigned incorrectly. no pixels are visible.

The area below the ROC curve is referred to as AUC. The closer it is to one, the more effective the modelling is. Its value spans from 0.5 to 1.

RMSE and MAE Index

The discrepancy between measured and calculated values used to assess model accuracy is known as prediction error is the formula for the RMSE and MAE indices. (8) and (9).

Eq (8)

$$RMSE = \sqrt{\frac{\sum_{i=1}^n (y_i - \bar{y}_i)^2}{N}}$$

Eq (9)

$$MAE = \frac{\sum_{i=1}^n |(y_i - \bar{y}_i)|}{N}$$

where N is the total number of training data, \bar{y}_i is the observed value, y_i is the predicted value, and y_i is the predicted value.

Sensitivity analysis

The impact of changing model inputs on model results is demonstrated by sensitivity analysis. The requirement for their presence or absence is established by the elimination of one of the relevant criteria. Equation is used to perform sensitivity analysis (10).

$$RD = \frac{AUC_{all} - AUC_i}{AUC_{all}} * 100$$

where AUCall is the training data's final AUC value when all parameters are present, and AUCi is the training data's final AUC value when parameter I is absent. RD is the relative decrease index.

IV. RESULTS



Spatial autocorrelation result

The Moran's I and Getis- Ord Gi* index results are shown in Table-1. As a result, the research area had concentrations of asthma cases. The autocorrelation test results are statistically significant despite the small P-value parameter, demonstrating that the criteria of the null hypothesis are met in light of the observed data and that the distribution of diseases is not random. Spatial clusters using the Moran's I index and Getis Ord Gi* index are shown in Figures 3 and 4, respectively. Disease clusters are indicated by high-high and hotspot regions. Clusters of no-disease are found in low-low and cold spots.

Table 1- Results of the spatial autocorrelation indexes.

Index	Indexvalue	z-score	p-value	Distributiontype
Moran'sI	0.149	6.807	0.000	Clusterd
Getis-Ord Gi*	0.000028	2.673206	0.007514	Clusterd

Figure 3. Spatial clusters using the Moran's I index.

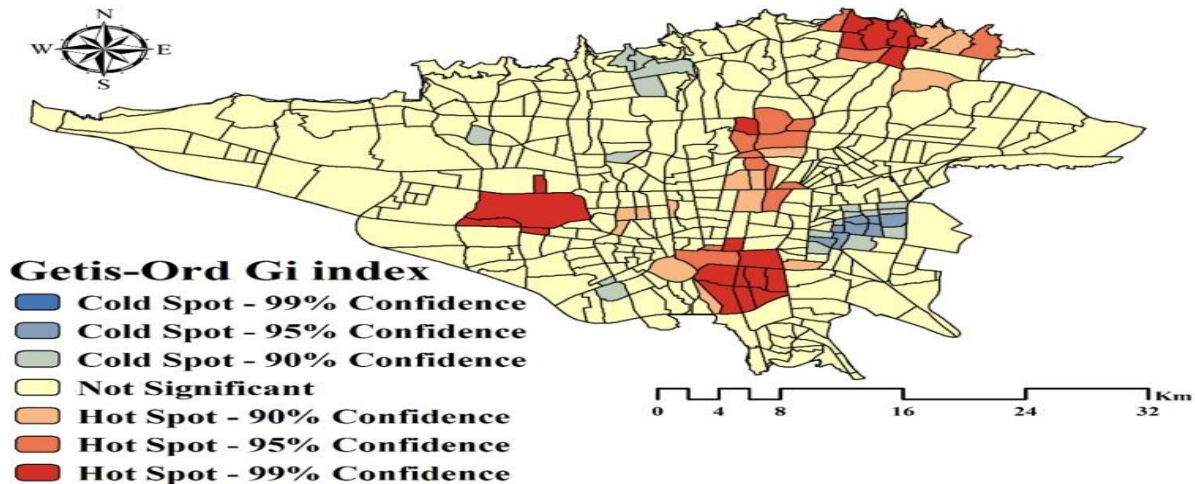
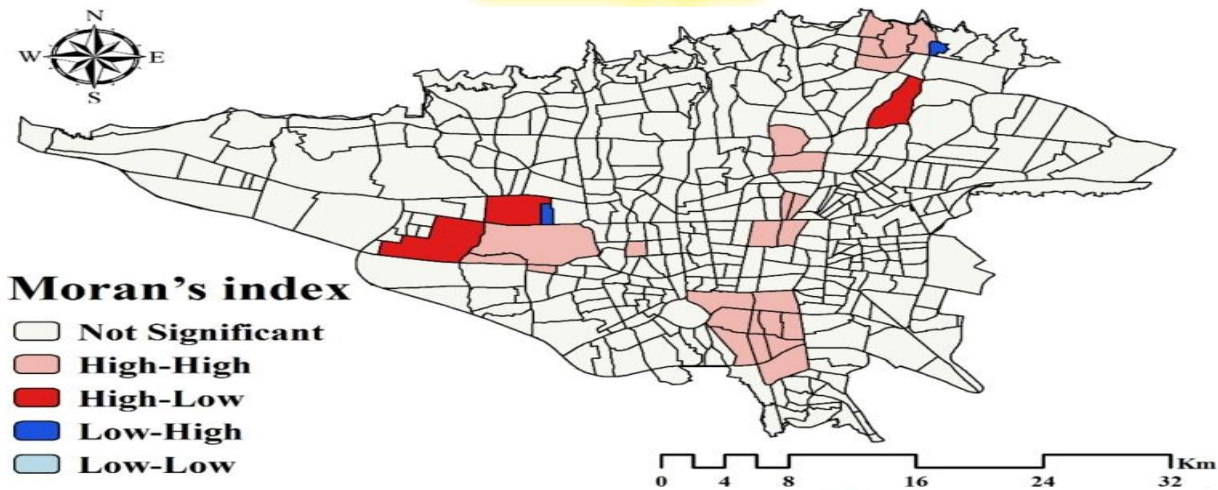


Figure 4. Spatial clusters using the Getis-Ord Gi*

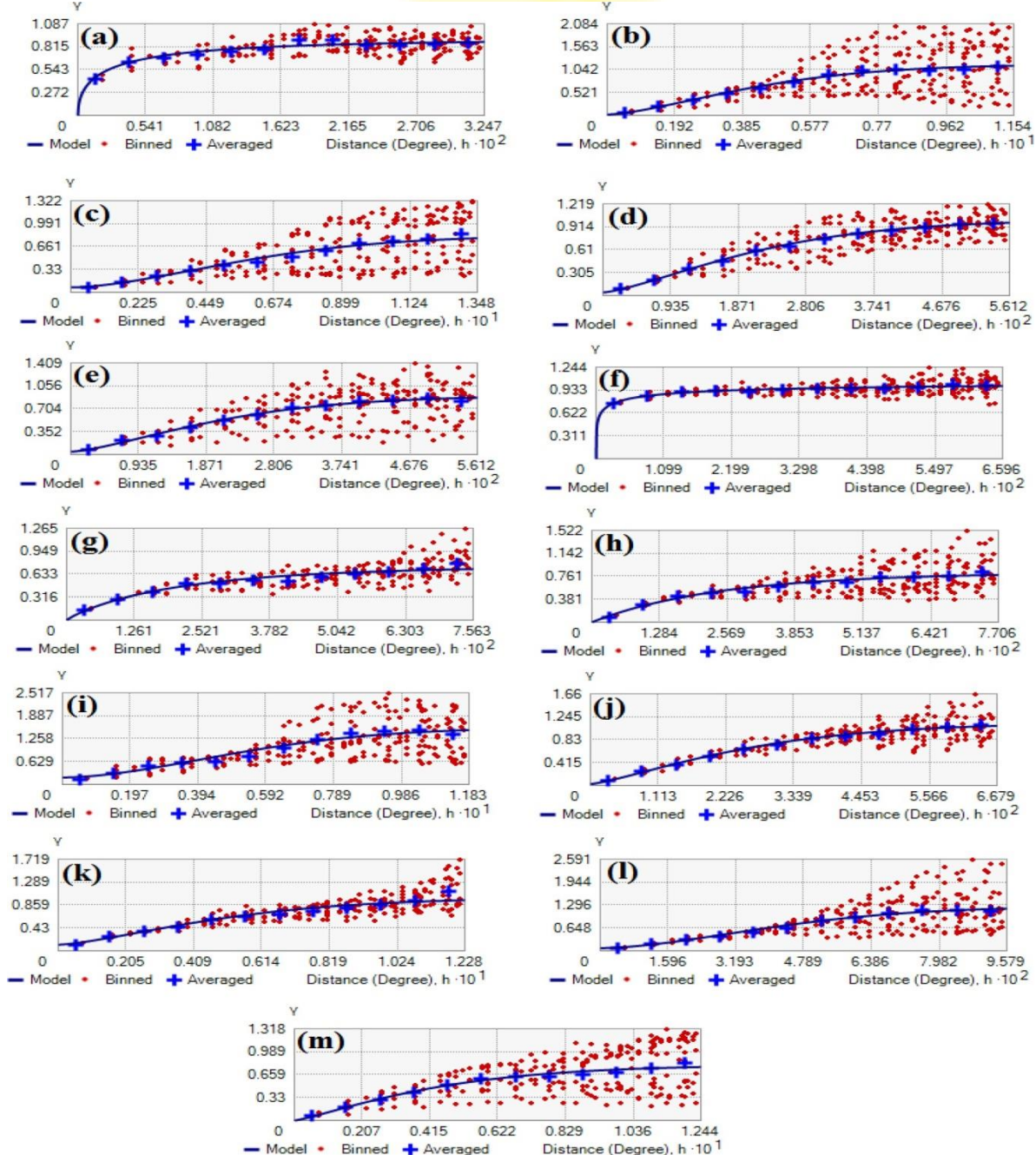
Table 1 displays the Moran's I and Getis- Ord Gi* index results. As a result, there were concentrations of asthma cases in the study region. Despite the tiny P-value parameter, the autocorrelation test results are statistically significant, indicating that the null hypothesis is supported by the observed data and that the distribution of diseases is not random. Figures 3 and 4, respectively, display spatial clusters using the Moran's I index and Getis Ord Gi* index. High-high and hotspot areas are indicators of disease clusters. Low-low and frigid spots are where no-disease clusters are identified.

Table2- Results of the semi variogram parameters.



Criterion	Nugget	Range	PartialSill	SD
Distancetostreet	0	0.02585	0.90347	0%
Pressure	0.020703	0.10298	1.143515	1.77%
Windspeed	0.0723	0.13484	0.746103	8.83%
Humidity	0.04172	0.053865	0.968473	4.12%
Temperature	0.04508	0.051281	0.85825	4.99%
Distancetopark	0	0.06541	1.041133	0%
PM2.5	0	0.075632	0.73868	0%
PM10	0	0.077056	0.824453	0%
SO2	0.193513	0.11833	1.36949	12.38%
NO2	0.028775	0.066788	1.107712	2.53%
CO	0.11694	0.122836	0.877	11.76%
O3	0.079762	0.095789	1.17747	6.34%
Rainfall	0	0.080033	0.80033	0%

Figure 5. Semi-variogram output. a street distance, b pressure, c wind speed, and d humidity Temperature (e),





(f) Parking distance, (g) "PM 2.5," (h) "PM 10," (i) "SO₂," (j) "NO₂," (k) "CO," (l) "O₃," and (m) "Rainfall." ArcGIS 10.3 (ESRI, Redlands, CA, USA, <http://www.esri.com>) was used to create this map.

DISCUSSION

Results from the spatial autocorrelation index in the study area demonstrated that environmental factors influenced disease occurrence and that asthma was not distributed randomly. Semi-variogram results between criteria affecting asthma showed that distance to parking, distance to road, PM 2.5, PM 10, and precipitation criteria exhibited the largest geographical dependence, followed by SO₂, CO, and O₃. Those were the criteria that were least spatially dependent.

According to the results of the range parameter, the criterion for road distance, temperature, and humidity showed the greatest spatial variability, whereas the criteria for wind speed, CO, and SO₂ showed the least regional variability. According to autocorrelation studies, every characteristic that affected asthma had a significant geographical relationship with it.

The requirements for PM 2.5 and PM 10 compared to the criteria for parking lot and road distance, 10 had stronger geographic ties.

The results of the FR model show that asthma attacks are more likely to occur close to a road. According to the findings of the FR model, geographical correlation, and RF model, the distance-to-road criterion had a substantial impact on the incidence of asthma in the study area. This is a result of the street's high volume of traffic and its close proximity to industrial areas.

According to spatial correlations between the two variables, an increase in PM 10 criteria was linked to an increase in the likelihood of asthma attacks. FR and the incidence of asthma attacks increase together with an increase in PM 2.5 levels. Under the authorised levels of air pollution, PM 2.5 and PM 10 had a substantial geographic relationship with the likelihood of asthma episodes in the study area, according to the results of the FR, spatial autocorrelation, and RF models. PM 2.5 and PM 10 are typically produced by fossil fuel activities, such as those involving oil, gas, and coal, vehicle traffic, metal smelting and processing, and power plants. PM 2.5 particles enter the lungs deeply and remain suspended in the air for a longer time. The CO criterion results showed a correlation between higher FR. Along with an increase in PM 2.5 levels, FR and the frequency of asthma attacks rise.

According to the outcomes of the FR, spatial autocorrelation, and RF models, PM 2.5 and PM 10 demonstrated a significant geographic association with the likelihood of asthma episodes in the research area under the permitted levels of air pollution. Fossil fuel-related operations, such as those using oil, gas, and coal, vehicle traffic, metal smelting and processing, and power plants, are typically responsible for the production of PM 2.5 and PM 10. Deeply penetrating PM 2.5 particles hang around in the air for a longer period of time.

Results from the CO criteria revealed a link between higher FR. This criterion could not have modelled asthma without significant climatic change in the study area because the rate of asthma episodes increased with rising SO₂ levels. Sulfur dioxide is more likely to enter the respiratory system when inhaled because it is more soluble in water than other contaminants. Asthma attacks were more common in middle class people, according to the NO₂ criterion results. Storms and climate change that result from changes in barometric pressure can indirectly affect asthma and air pollution. The likelihood of asthma attacks increased in the study area as air pressure rose. According to the results based on wind speed, FR and the frequency of asthma attacks are inversely related. It therefore had no effect on asthma modelling in the research area. Strong winds can spread dust and pollutants. This criterion had little impact on the modelling of asthma-prone areas because of the low wind speeds in the research area. Humidity indirectly influenced asthma attacks. When these



criteria are raised, the levels of the secondary pollutants nitrates and sulphates rise. The results of the humidity criteria showed that at 40% relative humidity, the likelihood of asthma episodes in the research area was increased. Precipitation criteria and asthma attack frequency were inversely associated. The quantities of air pollutants and the associated chemical processes decreased as precipitation increased. Precipitation results indicate that asthma is more likely to develop in the middle layer (303-340 mm) of this baseline. It was located that there were

There are geographical relationships between temperature and the occurrence of asthma, with a higher risk of development at 15 °C. Temperature increases frequently cause an increase in ozone levels and photochemical reactions. The results regarding parking distance showed that there was a substantial spatial association between this criterion and the amount of asthma in the study area. Being adjacent to a city park is good for one's health since it encourages social interaction, physical activity, and stress relief. The results showed that the distance from the parking lot increased the risk of an asthma attack in the study area.

The results showed that the RF model was quite accurate in mimicking asthma in the research location. In order to minimise over-fitting, the RF model's output findings used the average of many decision trees to build a smaller tree using a random subtree of features. The accuracy remained high even without data scaling, so it was not necessary for the HF model to have scaling capabilities.

CONCLUSION

This study used RF models to pinpoint Tehran, Iran's asthma-prone neighborhoods. The following are the results of our investigation: Asthma was strongly correlated with the distance to the closest parking lot, the distance to the nearest road, the PM 2.5 level, and the PM 10 level, according to the results of the spatial autocorrelation. Based on the results of the FR model, the following parameters were calculated: 100–200 m to the road, PM 10 >93.24, PM 2.5 between 31–76 and 34.1, CO >2.98, O3 12.75–17.98, SO2 >17.89 20.77, NO2 4962–56.08, pressure 1009.69–1010.17, wind speed 14.002–15.004, humidity 40.48–41.59, temperature 15.6–16.07, precipitation. Findings from the RF model show that the distance to the parking lot, the distance to the road, the PM 2.5, and the PM 10 criteria had the greatest impact on the modelling of the asthma territory. The results showed that the RF model performed well in the area with a high prevalence of asthma. The use of GIS-created disease risk maps can aid in the management, control, and prevention of diseases.

References

- [1] A. K. Sharma, A. Nandal, A. Dhaka and Rahul Dixit, "A survey on machine learning based brain retrieval algorithms in medical image analysis," *Health and Technology*, vol. 10, pp. 1359–1373, August 6, 2020.
- [2] K. Gautam, V. K. Jain, S. S. Verma, "Identifying the Suspect nodes in Vehicular Communication (VANET) Using Machine Learning Approach", *Test Engineering & Management*, vol. 83, no. 9, pp 23554-23561, March-April 2020.
- [3] A.K. Sharma et al., "HOG transformation based feature extraction framework in modified Resnet50 model for brain tumor detection," *Biomedical Signal Processing and Control*, vol 84, 2023.
- [4] Gautam, K., Jain, V.K., Verma, S.S., Vyas, S. (2023). Vehicular Communication Strategy Using Machine Learning and Image Processing to Enhance Observations and Control on the Road Side Area. In: Gunjan, V.K., Zurada, J.M. (eds) *Proceedings of 3rd International Conference on Recent Trends in Machine Learning, IoT, Smart Cities and Applications. Lecture Notes in Networks and Systems*, vol 540. Springer, Singapore. https://doi.org/10.1007/978-981-19-6088-8_34
- [5] A. K. Dubey, A. Kumar, V. García-Díaz, A. K. Sharma and K. Kanhaiya, "Study and analysis of SARIMA and LSTM in forecasting time series data," *Sustainable Energy Technologies and Assessments*, vol. 47, 2021.



- [6] K. Gautam, V.K. Jain, S. Verma, "A Survey on Neural Network for Vehicular Communication", Mody University International Journal of Computing and Engineering Research, vol. 3, no. 2, pp. 59-63, 2019.
- [7] K. Kanhaiya, R. Gupta and A. K. Sharma, "Cracked cricket pitch analysis (CCPA) using image processing and machine learning," *Global Journal on Application of Data Science and Internet of Things*, vol. 3, no. 1, pp. 11-23, 2019.
- [8] K. Gautam, S. S. Verma and V. K. Jain, "Enhancement in the Reliability of Vehicular Communication System for Road Side Area," *2022 International Mobile and Embedded Technology Conference (MECON)*, 2022, pp. 639-644, doi: 10.1109/MECON53876.2022.9752226
- [9] S. Sharma, A. K. Sharma, "An adaptive approach for Decomposition of Space Variant Blur and It's Restoration using Blind Deconvolution," *International Journal for research & Development in Technology*, vol. 7, no. 4, pp. 492-496, April 2017.
- [10] K. Agarwal, G. K. Soni, and K. Gautam, "Flipped Voltage Follower Based Operational Transconductance Amplifier For High Frequency Application" *International Journal of Advanced Science and Technology*, vol. 29, no. 9, pp. 8104-8111, 2020.
- [11] Sharma, A.K.; Nandal, A.; Dhaka, A.; Koundal, D.; Bogatinoska, D.C.; Alyami, H. Enhanced Watershed Segmentation Algorithm-Based Modified ResNet50 Model for Brain Tumor Detection. *BioMed Res. Int.* 2022.
- [12] K. Gautam, S.S. Verma, "A Review on Vehicular Communication System", *A Journal of V., S. Sancheti, A. Dhaka, A. Nandal, H. G. Rosales, D. Koundal, F. E. L. Monteagudo, C. E. G. Tajada, A. K. Sharma. "Lambertian Luminous Intensity Radiation Pattern Analysis in OLOS Indoor Propagation for Better Connectivity" [Wireless Communications and Mobile Computing, 2022.](#)*
- [13] K. Gautam, S.S. Verma, "A Latest Development and Opportunity in VANET", *Mody University International Journal of Computing and Engineering Research*, vol 2, no. 1, pp. 45-48, 2018.
- [14] A.K. Sharma, S. Jain, C. Goyal, "A Review on Object Detection With Deep Learning" *Mody University International Journal of Computing and Engineering Research*, Vol 3, No 2. [Pages: 90-97](#), 2019.
- [15] S. Pathak, S. Tiwari, K. Gautam, J. Joshi. "A Review on Democratization of Machine Learning In Cloud", *International Journal of Engineering Research and Generic Science*, vol. 4, no. 6, pp. 62-67, 2018.
- [16] N. Bhargava, A. K. Sharma, A. Kumar and P. S. Rathoe, "An adaptive method for edge preserving denoising," In *2017 2nd International Conference on Communication and Electronics Systems (ICCES)*, 2017, pp. 600-604.
- [17] K. Gautam, V. Sharma, R. Mishra, "Drone 2 Drone Communication: A Review", *International Journal on Future Revolution in Computer Science & Communication Engineering*, vol. 4, no. 1, pp. 150-153, 2018.
- [18] A.K. Sharma, A. Nandal, L. Zhou, A. Dhaka, T. Wu, "Brain Tumor Classification Using Modified VGG Model-Based Transfer Learning Approach" vol. 337, pp. 538 – 550, 2021.
- [19] A. K. Sharma, K. Kanhaiya and J. Talwar, "Effectiveness of Swarm Intelligence for Handling Fault-Tolerant Routing Problem in IoT," in *Swarm Intelligence Optimization: Algorithms and Applications*, A. Kumar, P. S. Rathore, V. G. Diaz and R. Agrawal, Eds. Wiley Online Library: John Wiley & Sons Inc., Dec. 2020, pp- 325-341.
- [20] A. K. Sharma, A. Nandal, A. Dhaka and R. Dixit, "Medical Image Classification Techniques and Analysis Using Deep Learning Networks: A Review," in *Health Informatics: A Computational Perspective in Healthcare*, R. Patgiri, A. Biswas and P. Roy, Eds. Singapore: Springer, January 31, 2021, vol. 932, pp. 233-258.
- [21] Arpit Kumar Sharma, Arvind Dhaka, Amita Nandal, Akshat Sinha and Deepika Choudhary, "Location-Based Internationalization and Localization With Mobile Computing" in *Emerging Trends in IoT and Integration with Data Science, Cloud Computing, and Big Data Analytics*, Eds. IGI Global, 2022, pp. 39-58.